Article

Red Ginseng Marc Oil Inhibits iNOS and COX-2 via NFκB and p38 Pathways in LPS-Stimulated RAW 264.7 Macrophages

Min-Ji Bak [1,†], Soon-Gi Hong [2,†], Jong-Won Lee [2] and Woo-Sik Jeong [1,*]

[1] Department of Food & Life Sciences, College of Biomedical Science & Engineering,
   Inje University, Gimhae 621-749, Korea; E-Mail: redapplemj@hanmail.net
[2] Ginseng Product Research Institute, R&D Headquarters, Korea Ginseng Corp., Daejeon 305-805,
   Korea; E-Mails: skhong@kgc.or.kr (S.-G.H.); insamlee@kgc.or.kr (J.-W.L.)

[†] These authors contributed equally to this work.

[*] Author to whom correspondence should be addressed; E-Mail: jeongws@inje.ac.kr;
   Tel.: +82-55-320-3238; Fax: +82-55-320-0691.

Abstract: In this study, we investigated the anti-inflammatory effects of red ginseng marc oil (RMO) in the RAW 264.7 macrophage cell line. RMO was prepared by a supercritical CO_2 extraction of waste product generated after hot water extraction of red ginseng. RMO significantly inhibited the production of oxidative stress molecules such as nitric oxide and reactive oxygen species in lipopolysaccharide (LPS)-activated RAW 264.7 cells. Levels of inflammatory targets including prostaglandin E2, tumor necrosis factor-α, interleukin (IL)-1β and IL-6 were also reduced after the treatment with RMO. In addition, RMO diminished the expressions of inducible nitric oxide synthase and cyclooxygenase 2 at both mRNA and protein levels. Blockade of nuclear translocation of the p65 subunit of nuclear factor κB (NFκB) was also observed after the treatment of RMO. Furthermore, RMO decreased the phosphorylations of p38 mitogen-activated protein kinase (MAPK) and its upstream kinases including MAPK kinases 3/6 (MKK3/6) and TAK 1 (TGF-β activated kinase 1). Gas chromatographic analysis on RMO revealed that RMO contained about 10% phytosterols including sitosterol, stigmasterol and campesterol which may contribute to the anti-inflammatory properties of RMO. Taken together, these results suggest that the anti-inflammatory effect of RMO in LPS-induced RAW 264.7 macrophages could be associated with the inhibition of NFκB transcriptional activity, possibly via blocking the p38 MAPK pathway.

1. Introduction

Inflammation, a biological response to physical or chemical injurious stimuli, is closely associated with the release of *pro*-inflammatory mediators such as inducible nitric oxide synthase (iNOS), cyclooxygenase-2 (COX-2), and *pro*-inflammatory cytokines such as interleukins (ILs) and tumor necrosis factor α (TNF-α) [1]. The expression of these inflammation-related genes is controlled by the intracellular signaling pathways such as nuclear factor κB (NFκB) and mitogen-activated protein kinases (MAPKs) at both transcriptional and post-transcriptional levels [2,3].

NFκB is a pivotal transcription factor regulating various genes expression involved in immune and acute phase inflammatory responses [4]. The transcription factor NFκB forms a cytoplasmic complex with its inhibitors, IκBs, under normal physiological conditions. Stimulation of inflammatory cells with lipopolysaccharide (LPS), TNF, irradiation or viral infection results in the activation of Toll-like receptor 4 and downstream inhibitor κB kinases (IKKs) which in turn phosphorylates IκB and leads to NFκB translocation into the nucleus where it regulates transcription of its target genes [5]. Recently, many studies have demonstrated the roles of phytochemicals in anti-inflammatory activity through down-regulation of the NFκB pathway [6–9].

Activation of the NFκB signaling pathway is closely linked to the activations of MAPKs, which activate downstream transcription factors that promote inflammatory gene expression [10,11]. Furthermore, MAPKs are phosphorylated by upstream MAPK kinases (MAPKKs), which are dual specificity kinases that can phosphorylate threonine and tyrosine residues, and MKKs are in turn activated by MAPK kinase kinases (MAPKKKs), which are related to serine/threonine protein kinases [12]. These activated transcription factors regulate various *pro*-inflammatory cytokines and mediator factors regulate various *pro*-inflammatory cytokines and mediator genes including iNOS, COX-2, interleukin and TNF-α [13–15].

Ginseng (*Panax ginseng*) has been used as a traditional remedy in oriental medicine. Ginseng in Korea is classified into three categories, including fresh, white and red ginseng [16]. Red ginseng has been heat steamed and dried. As a consequence of this process, red ginseng undergoes certain biochemical chances and acquires certain pharmacological properties such as antioxidant [9], anti-viral [17], anti-aging [18], anti-depressant [14], anti-obesity [19], anti-carcinogenic [20] and hepatoprotective [21] effects. These beneficial effects of red ginseng have been mostly studied using its water-soluble fractions, probably because red ginseng is widely consumed in the form of hot-water extract or its concentrates. Therefore, we prepared red ginseng marc oil (RMO) by supercritical CO_2 extraction of waste-products generated after hot water extraction of red ginseng. In recent years, there has been an increasing interest in extracted essential oils and lipid-soluble bioactive compounds from various herbs and plants compared to water-soluble bioactive compounds. Newly discovered properties of essential oils include antibacterial [22], antifungal [23], antiobesity [24], antioxidant [25] and anti-inflammatory activities [26]. The pharmacological properties of essential oils extracted from plants have been the

focus of interest from both academia and the pharmaceutical industry. Recently, our research group documented the antioxidant and hepatoprotective effects of RMO in H_2O_2-treated HepG2 cell and CCl_4-treated mice [27]. In the present study, we show that RMO from red ginseng byproducts has anti-inflammatory activity and elucidate its underlying molecular mechanism for the first time in LPS-induced RAW264.7 cells.

2. Results and Discussion

2.1. Effects of RMO on Cell Viability

The cytotoxic effects of RMO in RAW 264.7 cells were evaluated using the 3-(4,5-dimethylthiazol-2-yl)-2,5-diphenyltetrazolium bromide (MTT) assay. As shown in Figure 1, RMO did not affect cell viability for 48 h at concentrations up to 200 μg/mL. For the subsequent experiments described in this study, non-toxic dose range (10 to 100 μg/mL) of RMO was used.

Figure 1. Effects of RMO on LPS-induced RAW264.7 cell viability. Cells were treated with different concentrations of RMO for 48 h, and cell viabilities were determined by MTT assay.
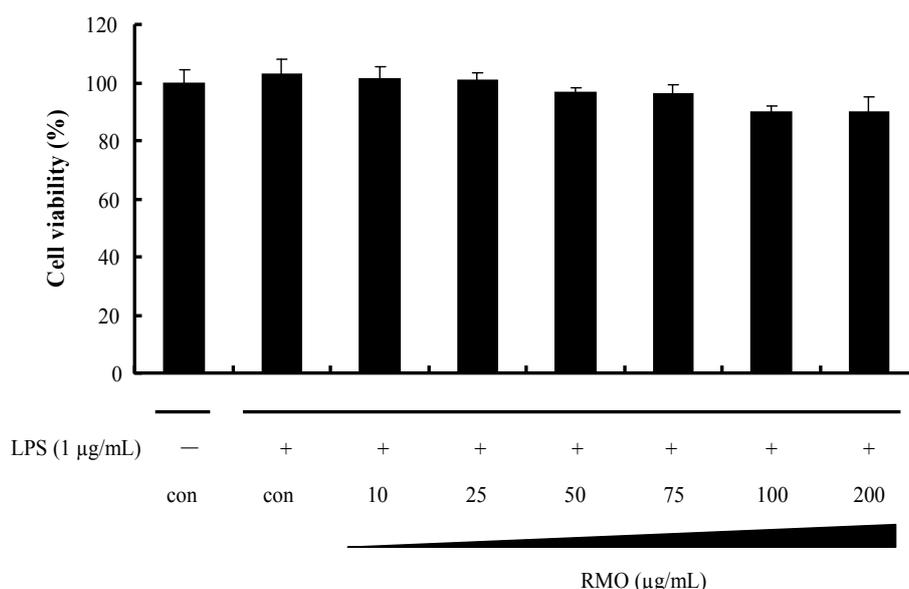
2.2. RMO Inhibits NO and PGE₂ Production by Suppressing the Expression of iNOS and COX-2 in LPS-Stimulated RAW 264.7 Cells

The inflammatory products NO and PGE_2 can be induced by the expression of iNOS and COX-2, respectively, as a part of the innate immune system, and the inhibition of NO and PGE_2 over-production might be used as a therapeutic tool to treat inflammatory diseases [28]. Since there is a causal relationship between inflammation and cancer, iNOS and COX-2 are often considered as potential molecular targets for chemoprevention [29]. To examine whether RMO can suppress the inflammatory response, the inflammatory responses were induced in RAW 264.7 cells by LPS treatment. As shown in Figure 2A,B, treatment of the cells with LPS dramatically increased NO and PGE_2 productions; however, RMO significantly inhibited the production of these inflammatory molecules in a dose-dependent manner.

Figure 2. RMO inhibits LPS-induced NO and PGE$_2$ productions and iNOS and COX-2 expressions in RAW 264.7 cells. Cells were pretreated with RMO (10, 25, 50 and 100 μg/mL) for 1 h and then exposed to 1 μg/mL of LPS for 24 h. (**A**) The culture medium was subsequently collected, and the nitrite concentration was measured by the Griess reaction. (**B**) Each culture supernatant was subsequently collected, and the amount of PGE$_2$ released was measured using the PGE$_2$ Parameter Assay Kit. Data are presented as the means ± S.D. of three independent experiments. *, # Significantly different from the no treatment and LPS-treated control, respectively ($p < 0.05$). Aspirin (ASP) was used as a positive control. (**C**) Treatment of RAW 264.7 cells with RMO for 1 h followed by stimulation with LPS (1 μg/mL) for 24 h in the continued presence of RMO. Then the cells were harvested and whole cell extracts were prepared for Western blot analysis for the indicated proteins. (**D**) The cells were treated with RMO for 1 h, then stimulate with LPS for 24 h, mRNA of iNOS and COX-2 were measured by RT-PCR. The results are expressed as the means ± S.D. for three separate experiments, each with three replicates.
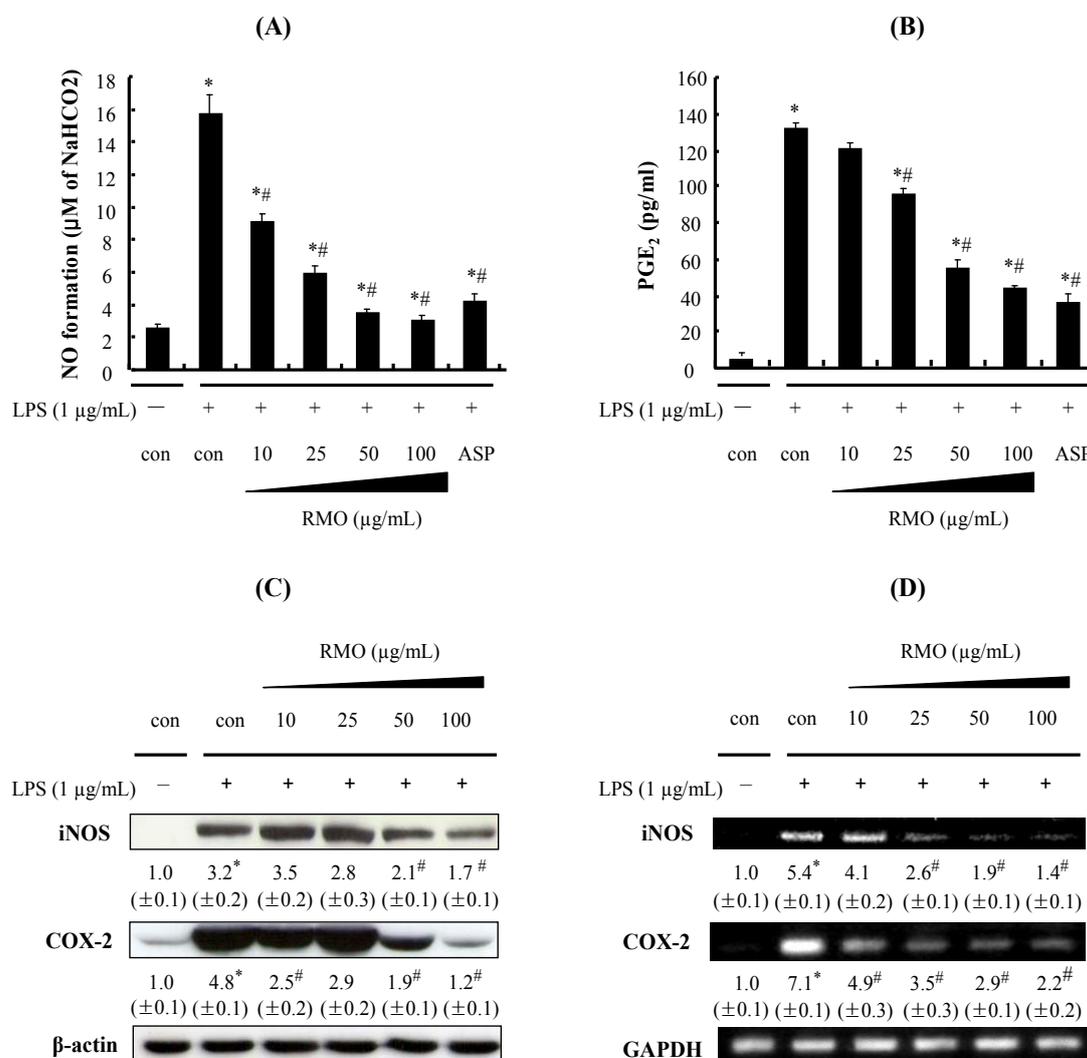
In particular, NO production decreased to near basal levels when the cells were treated with the highest concentration of RMO (100 μg/mL). In addition, RMO treatment at the doses over 50 μg/mL displayed stronger inhibition on NO production than the positive control aspirin, a well-known

anti-inflammatory drug. The expressions of inflammatory enzymes iNOS and COX-2 were also strongly induced by LPS treatment while these over-expressions were suppressed by RMO in a concentration-dependent manner both at protein and mRNA levels (Figure 2C,D). Although there seems to be a dose-dependent tendency by RMO treatments in the expressions of these genes, the expression levels of protein and mRNA are not exactly same. The reason for this is not clear at this moment, but there might be an involvement of translational or post-translational modification of these genes and further studies are needed to elucidate the exact mechanisms. Anti-inflammatory agents decreasing NO and PGs productions by simultaneously inhibiting the iNOS and COX-2 genes have been considered to have a potentially therapeutic effect in the treatment of inflammatory and infectious diseases [30,31]. Our results suggest that RMO might inhibit the production of NO and PGE_2 by down-regulating the expression of iNOS and COX-2, which could be activated by inflammatory stimuli such as LPS.

### 2.3. RMO Inhibits the Protein Expression of Pro-Inflammatory Cytokines in LPS-Stimulated RAW 264.7 Cells

Certain cytokines such as TNF-α, IL-1β and IL-6 have *pro*-inflammatory effects both *in vitro* and *in vivo* [32,33]. Moreover, TNF-α production is crucially required for the synergistic induction of NO synthesis in IFN-γ- and/or LPS-stimulated macrophages [34]. TNF-α elicits a number of physiological effects such a septic shock, inflammation, cachexia and cytotoxicity; IL-6 is believed to be an endogenous mediator of LPS-induced fever [35]. Therefore, the inhibition of the *pro*-inflammatory cytokines has been identified as targets for anti-inflammatory therapies. Since RMO was found to potently inhibit the *pro*-inflammatory mediators NO and PGE_2, we investigated its effects on LPS-induced TNF-α, IL-1β and IL-6 releases; this was done by enzyme immunoassay (EIA) and Western blot. As shown in Figure 3A,B, RMO concentration-dependently reduced the production of TNF-α, IL-1β and IL-6 and the corresponding protein expression levels.

### 2.4. RMO Suppresses IKK/IκB/NFκB Signals and NFkB Nuclear Translocation in LPS-Induced in LPS-Stimulated RAW 264.7 Cells

Extracellular stimuli including LPS induce IKK/IκB/NFκB pathway to stimulate the production of inflammatory cytokines and *pro*-inflammatory enzymes [36–38]. iNOS and COX-2 genes are known to contain NFκB-binding sites in their promoter region [39]. Under unstimulated condition, NFκB is sequestered in the cytosol, associated with the inhibitory IκB protein. The activation of IKKs in response to extracellular stimuli leads to rapid phosphorylation and degradation of IκB, which makes NFκB translocate to the nucleus where it regulates gene transcription [40–42]. We examined whether the inhibitory effects of RMO on the production of inflammatory markers including NO, PGE_2, TNF-α, IL-1β and IL-6 are related to its blockade of the NFκB signaling pathway. Thus, we first assessed regulatory ability of RMO on the phosphorylation of p65 and IκBα. As illustrated in Figure 4A, LPS strongly induced the phosphorylation of p65 and IκBα whereas RMO dose-dependently inhibited these phosphorylations. Phosphorylation of the upstream kinase IKKα/β was also similarly diminished by RMO treatment but the protein level of IKKα/β was not affected by RMO. Therefore, RMO seems to

reduce the production of inflammatory markers through inhibiting phosphorylations of IKK/IκB/NFκB signaling pathways.

Figure 3. RMO inhibited the production of LPS-induced *pro*-inflammatory cytokine in RAW 264.7 cells. (**A**) RAW 264.6 cells were pretreated with RMO for 1 h, and then stimulated with LPS (1 μg/mL). Culture media were collected after 24 h in order to measured TNF-α and IL-6 concentrations using ELISA. Data are presented as the means ± S.D. of three independent experiments. *, # Significantly different from the no treatment and LPS-treated control, respectively ($p < 0.05$). (**B**) The cells were incubated with RMO in the presence or absence of LPS for 24 h. Then the cells were harvested and whole cell extracts were prepared for Western blot analysis for the indicated proteins. The results are expressed as the means ± S.D. for three separate experiments, each with three replicates.

(A)

(B)
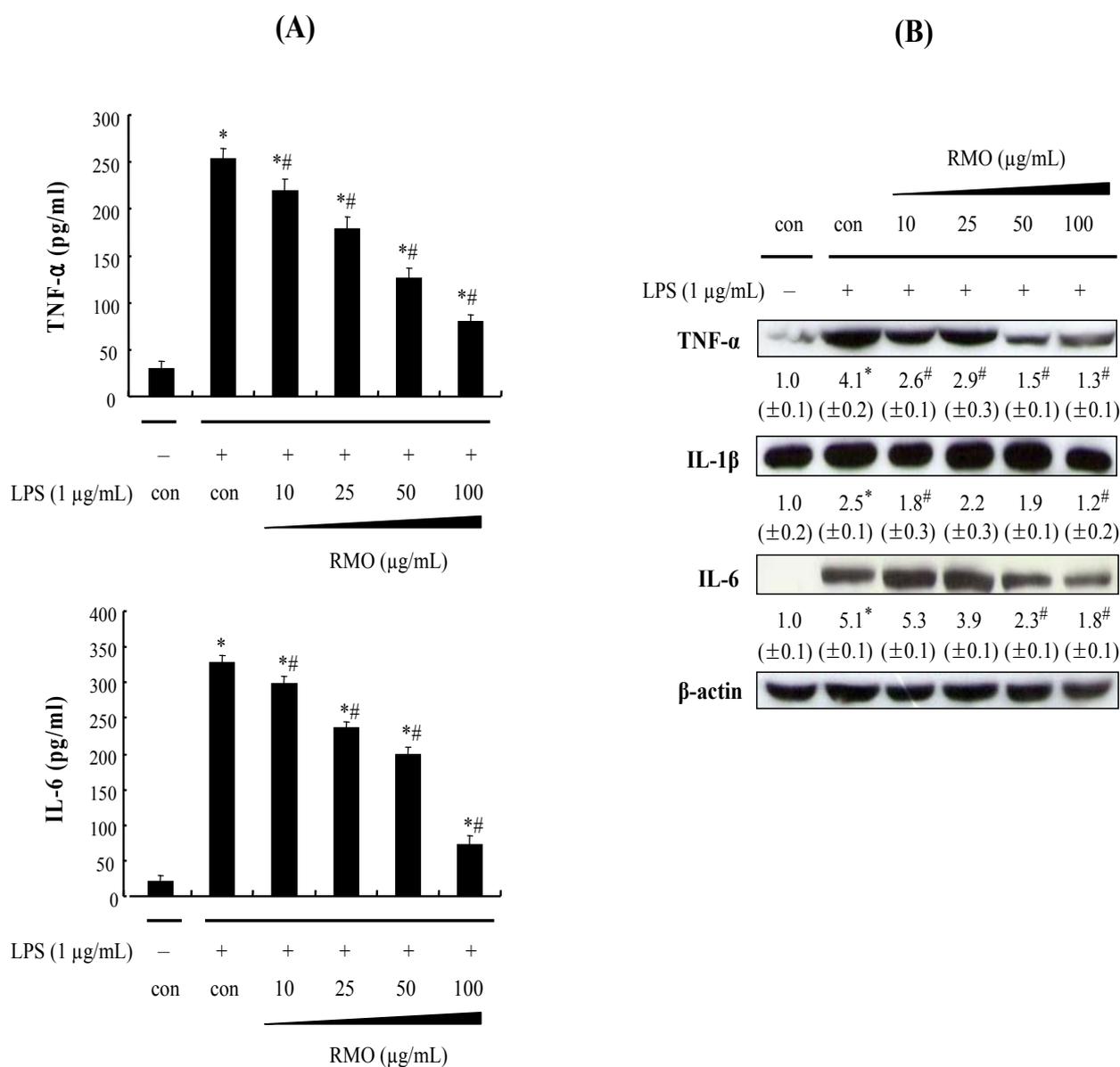
Figure 4. RMO suppresses NFκB activation by blocking NFκB p65 nuclear translocation in LPS-induced RAW 264.7 cells. (**A**) Cell were treated with RMO and stimulated with LPS. Then the cells were harvested and whole cells extracts were prepared for Western blot analysis for the indicated proteins. (**B**) Cells were pretreated with RMO for 1 h and then stimulated with LPS. The cells were harvested at 2 h, and then prepared nuclear extracts for the detection of phosphorylated NFκB p65 subunit and cytosolic extracts for the detection of phosphorylated IκBα by Western blot. (**C**) Cell were pretreated with RMO (100 μg/mL) for 1 h followed by stimulation with LPS for 2 h. Samples were stained by anti-p65 antibody and DAPI then prepared for confocal microscopy analysis. The results are expressed as the means ± S.D. for three separate experiments, each with three replicates. *, # Significantly different from the no treatment and LPS-treated control, respectively ($p < 0.05$).

(A)

(B)

(C)
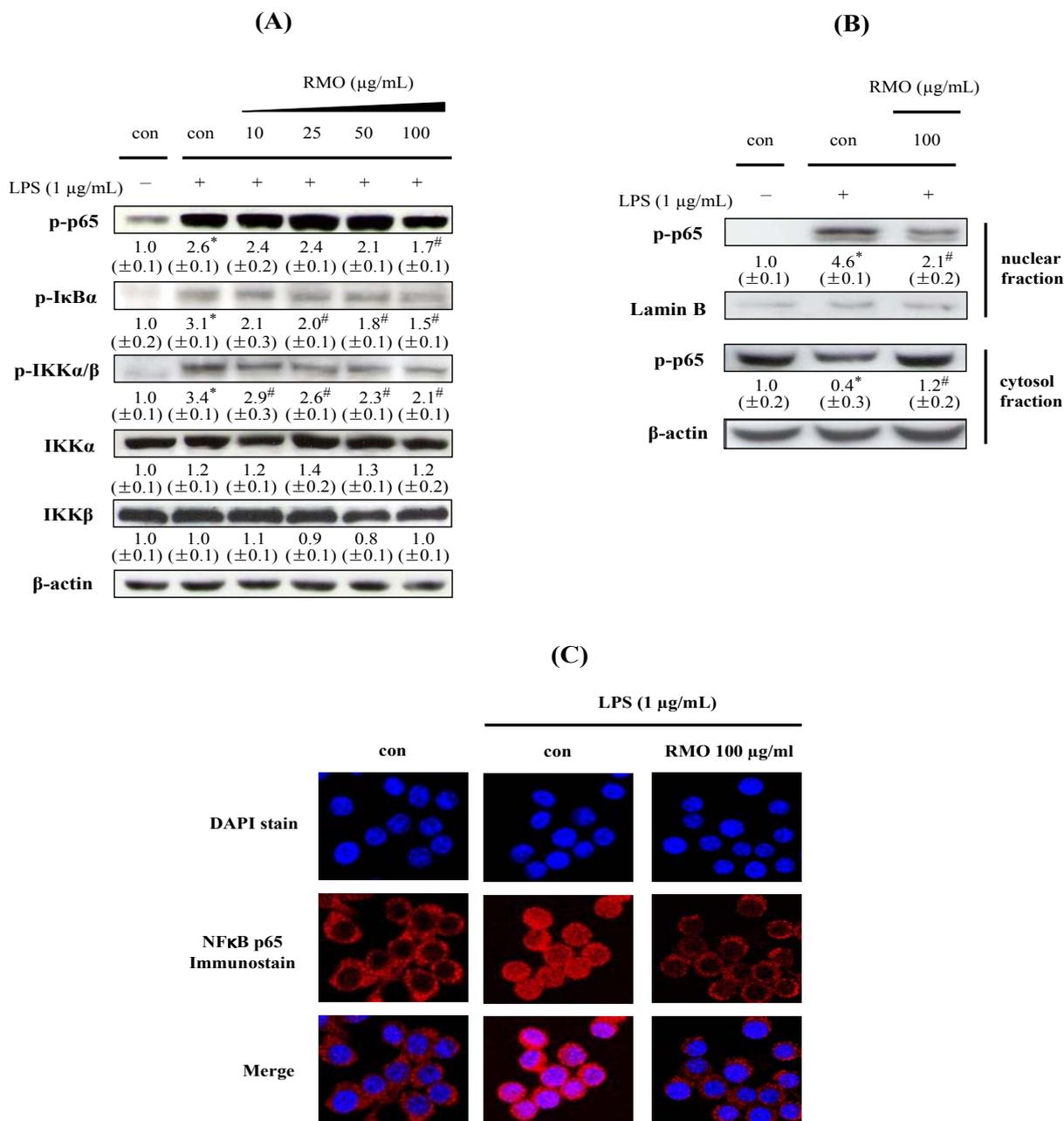
We next investigated whether RMO could inhibit the nuclear translocation of p65 after its release from IκB using Western blot and confocal microscopy analyses. Upon exposure of cells to LPS, p-p65 was accumulated in the nuclear fraction whereas the nuclear accumulation of p-p65 was reduced to less than half after RMO treatment (Figure 4B). For the cytosolic fractions, the results were opposite. These results were confirmed by immunofluorescence staining assay and the results are displayed in Figure 4C. Cytoplasmic retention of p-p65 was observed in cells treated with RMO, while translocation of p-p65 into the nucleus was observed in LPS-induced cells. Taken together, these results clearly demonstrate that RMO inhibits NFκB activation by preventing the LPS-stimulated nuclear translocation of p-p65 in RAW 264.7 cells. Many studies have suggested that certain phytochemicals could suppress inflammatory responses by regulating the NFκB pathway [43–45]. These findings concur with our finding that the transcriptional inhibition of *pro*-inflammatory mediators by RMO is associated with the IKK/NFκB signal pathway.

2.5. RMO Inhibits Phosphorylation of MAPK, MAPKK, and MAPKKK in LPS-Stimulated RAW 264.7 Cells

Various intracellular pathways are involved in inflammatory actions through up-regulating the production of major mediators on inflammation [46]. Three families of MAPKs including ERK, JNK and p38 play critical roles in cell growth regulation and differentiation and in the control of cellular responses to cytokines and stressors [47]. MAPK phosphorylation activates the transcription of NFkB-mediated *pro*-inflammatory cytokines [48]; Therefore, MAPKs are often considered as molecular targets for the development of novel anti-inflammatory phytochemical. We investigated MAPKs phosphorylations in the presence or absence of RMO in LPS-stimulated cells (Figure 5A). The phosphorylations of ERK, JNK, and p38 were elevated when cells treated with LPS alone. RMO exclusively repressed p38 phosphorylation but did not affect ERK and JNK phosphorylations. p38 pathway inhibition has been reported to decrease *pro*-inflammatory cytokines production in monocytes/ macrophages via transcriptional and post-transcriptional regulation [49].

Furthermore, the activation of MAPKs is known to require both tyrosine and theronine phosphorylation by the activated MAPKKs (MEK1/2, SEK1/MKK4, MKK7 or MKK3/6). Among the MAPKs, p38 MAPK is activated by dual phosphorylation on Thr180 and Tyr182 by upstream MAPK kinases: MAP2K6 or MAP2K3 (MKK3/6), which are activated by upstream MAPKKKs, and stimulated by a variety of stimuli. A MAPKK-independent mechanism of p38 activation involves transforming growth factor-β-activated protein kinase 1 (TAK1)-binding protein 1 (TAB1) [50,51]. To investigate the upstream kinases of p38 MAPK, we examined the modulatory effects of RMO on the phosphorylations of MAPKKs (MKK3/6, MEK1/2, MKK4, and MKK7) and MAPKKKs (TAK1, B-Raf, ASK1, and MLK3). RMO markedly suppressed the phosphorylations of MKK3/6 and TAK1 (Figure 5B,C), suggesting an involvement of RMO in TAK to MKK3/6 to p38 signaling pathways (Figure 6). Overall, our results imply that RMO might exert its anti-inflammatory ability through inhibiting p38 pathway which leads to NFκB inactivation and thereby suppressing expressions of inflammatory target proteins including proinflammatory cytokines and enzymes. Similar results have been reported with chemopreventive phytochemicals such as stercurensin [15], quercetin [52] and carnosol [53] which inhibit *pro*-inflammatory enzymes by targeting MAPK signaling pathways, including the p38 kinase pathway.

Figure 5. Effects of RMO on MAPK, MAPKK and MAPKKK phosphorylation in LPS-induced RAW 264.7 cells. Cells were treated with RMO for 1 h and stimulated with LPS (**A**) for 1 h, (**B**) 30 min, and (**C**) 15 min. Cell lysates were then subjected to Western blot analysis for the indicated proteins. The results are expressed as the means ± S.D. for three separate experiments, each with three replicates.

(A)

(B)

(C)
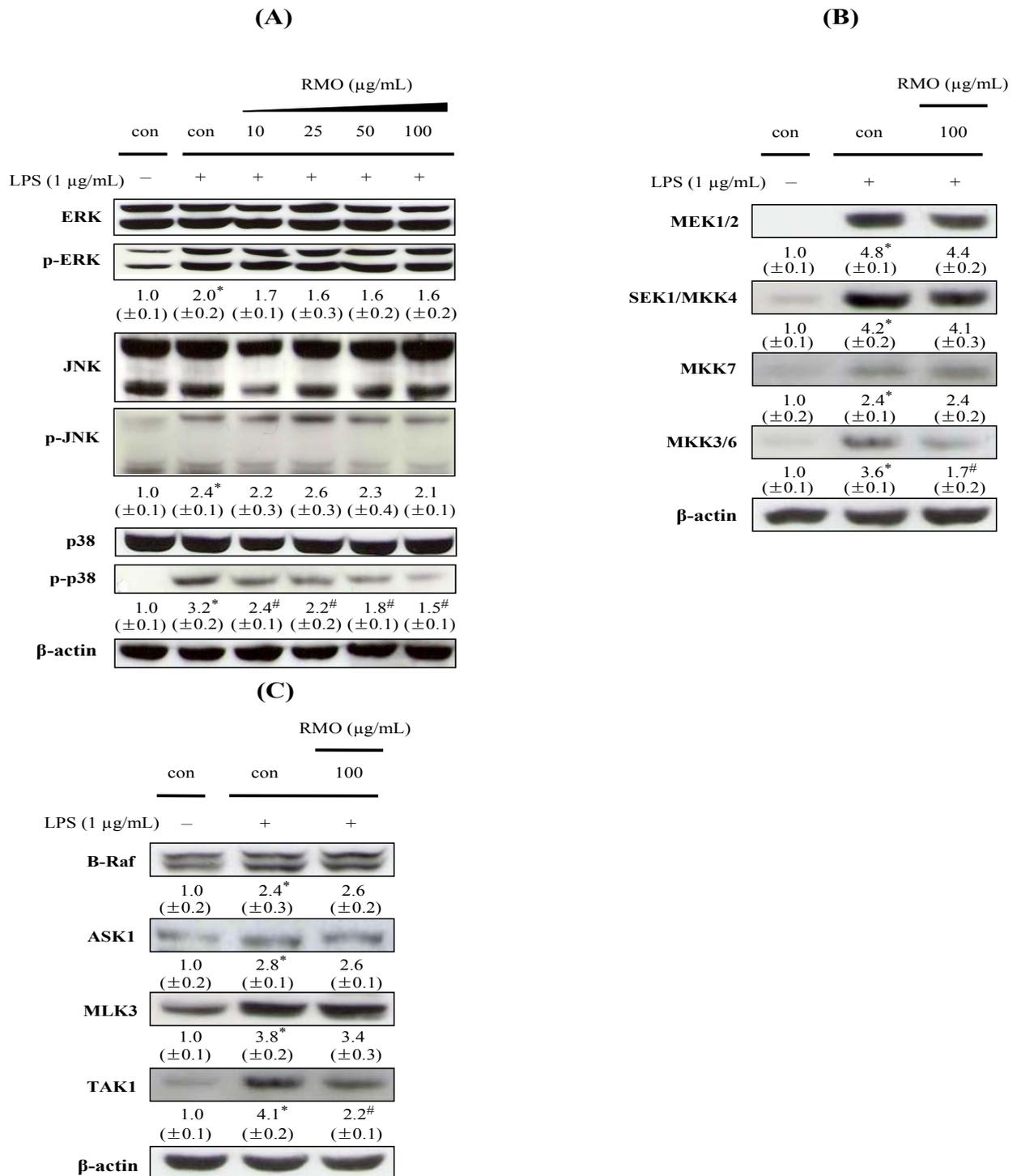
Figure 6. Schematic diagram illustrating the MAPK signaling cascades involved in RMO's inhibition of LPS-induced inflammation in RAW 264.7 cells.
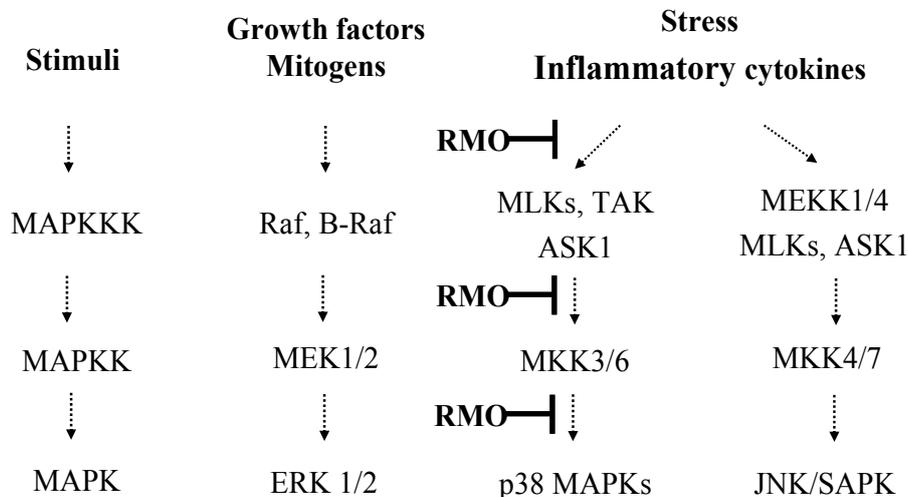
2.6. Phytosterols in RMO

Phytosterols are plant sterols that are found in seeds, roots, stems, branches, leaves and blossoms of various plants, including medicinal herbs, edible plants, shrubs and trees [54]. The three major phytosterols in plants include sitosterol, campesterol and stigmasterol [55]. It has been widely reported that phytosterols lower serum cholesterol level in animals and humans [54]. Besides the hypocholesterolemic effects, phytosterols have recently been reported to have anti-inflmmatory properties through the inhibition of proinflammatory cytokines including IL-6 and TNF-α [55]. As a part of investigations on active ingredients in RMO, we analyzed the content and composition of RMO using gas chromatography (GC) analysis. As shown in Table 1, RMO contained about 108 mg of phytosterols per g RMO and sitosterol was by far the most abundant phytosterol which accounts for 84% of total phytosterols in RMO. So far, only a few studies have reported phytosterols in ginseng. Sitosterol has been found from the fruit of ginseng [56]. Beveridge *et al.* have reported phytosterol content in the seed oil of American ginseng [57]. In the ginseng seed oil, sitosterol was the most abundant phytosterol followed by stigmasterol and campesterol. There has been no report on the phytosterol content or composition of red ginseng. Although there have been positive correlations between phytosterols and anti-inflammation, it is not clear whether the anti-inflammatory properties of RMO come from its phytosterols at this moment. More studies on the anti-inflammatory mechanisms of RMO phytosterols and studies on the presence of other possible active ingredients should be followed. Volatile compounds profiles, other than the phytosterols, of RMO are under investigation and to be reported separately.

Table 1. Phytosterol contents in red ginseng mark oil.

Phytosterol	Content (mg/g RMO)
Campesterol	3.9 ± 0.06
Stigmasterol	13.7 ± 0.27
Sitosterol	90.3 ± 2.58
Total	107.9 ± 2.91

3. Experimental

3.1. Chemicals

LPS (Escherichia coli O127:B8), Triton X-100 and all other chemicals were purchased from Sigma Chemical Co. (St. Louis, MO, USA).

3.2. Preparation of RMO

The supercritical CO_2 extract preparation was performed according to our previous report with some modifications [27]. In brief, dried red ginseng byproduct powder was placed into the extraction vessel of a pilot-scale supercritical fluid extraction system (Ilshin Autoclave Co., Ltd., Daejeong, Korea). Extractions with supercritical CO_2 were operated at 6,500 psi (relative to 450 bar) in combination with temperature at 65 °C. Extracted constituents were collected in a vial that was prefilled with a trapping solvent and maintained at 4 °C during the extraction step.

3.3. Cell Cultures

RAW264.7 murine macrophage cells were purchased from American Type Culture Collection (ATCC, Rockville, MD, USA). Cells were cultured at 37 °C and 5% CO_2 in Dulbecco's modified Eagles's medium (DMEM) containing 10% FBS, 100 units/mL penicillin, 100 μg/mL streptomycin (Hyclone, Logan, UT, USA).

3.4. Analysis of Cell Viability

The MTT [3-(4,5-dimethylthioazol-2-yl)-5-(3-carboxy-methoxyphenyl)-2-(4-sulfophenyl)-2H-tetrazolium, inner salt] assay was performed with a CellTiter 96 aqueous nonradioactive cell proliferation assay kit (Promega Corp., Madison, WI, USA) according to the manufacturer's instructions. Briefly, the cells were plated on 24-well plates at a density of 1×10^5 cells/well. After 24 h of incubation, the cells were treated with different doses of each sample for 48 h. Then, media were removed, and culture media containing MTS and phenazine methosulfate solution were added. After 1 h, the absorbance was measured at 490 nm with a PowerWave XS microplate reader (BioTek Instruments, Inc., Winooski, VT, USA). The data was expressed as percent cell viability compared to the vehicle control.

3.5. Measurement of Nitrite Oxide Formation

Nitrite, as an indicator of NO synthesis, was determined in cell culture supernatants by the Griess reaction. Briefly, RAW 264.7 cells were plated at 1×10^5 cells/well in 24-well plates and incubated at 37 °C for 24 h and then treated with RMO with LPS. After incubation of cells for 24 h, the supernatants (0.1 mL) were added to a solution of 0.1 mL Griess reagent (1% sulfanilamide and 0.1% naphthyl ethylene diaminedihydrochloride in 5% H_3PO_4) to form a purple azo dye. Using $NaNO_2$ to generate a standard curve, nitrite production was measured by spectrophotometry at 550 nm using a microplate reader (BioTek Instruments, Inc.).

3.6. Measurement of PGE₂ Production

The amount of PGE$_2$ produced from endogenous arachidonic acid was measured using a PGE$_2$ Parameter Assay Kit (R&D Systems, Minneapolis, MN, USA). RAW264.7 cells (1×10^5 cells/well) were treated with different concentration of RMO for 1 h and stimulated with LPS for 24 h, the conditioned media was collected to perform PGE$_2$ enzyme immune-metric assay according to the manufacturer's protocol. The concentration of PGE$_2$ was calculated according to the equation obtained from the standard curve plot using PGE$_2$ standard solution in the EIA kit.

3.7. Measurement of TNF-α and IL-6 Production

RAW 264.7 cells were plated at 1×10^5 cells/well, and stimulated with LPS for 24 h in the presence or absence of RMO. Culture supernatants were collected and the amount of TNF-α and IL-6 was determined by EIA using a protocol supplied by Amersham (Amersham Pharmacia Biosciences, Piscataway, NJ, USA).

3.8. Total RNA Extraction and Reverse Transcriptase (RT)-PCR Analysis

After LPS stimulation (1 μg/mL) of RMO-exposed cells for 24 h, total RNA was isolated using TRIzol reagent (Invitrogen, Carlsbad, CA, USA) and reverse transcribed into cDNA using SuperscriptTM RNase H reverse transcriptase (Invitrogen) according to the manufacturer's recommendations. Subsequent PCR analysis was carried out with aliquots of the cDNA preparation using a PCR System (Corbett Research, Sydney, Australia). The PCR conditions were as follows: predenaturation at 94 °C for 30 s, annealing at 55 °C (COX-2 and GAPDH) or 59 °C (iNOS) for 30 s and extension at 72 °C for 30 s. The PCR products were visualized in 2% agarose gels and documented using a Gel-Doc EQ system (Bio-Rad, Hercules, CA, USA). The primer sequences were as follows: mouse iNOS, 5'-GCC TTC AAC ACC AAG GTT GTC TGC A-3' (sense), 5'-TCA TTG TAC TCT GAG GGC TGA CAC A-3' (anti-sense); mouse COX-2, 5'-CTG GTG CCT GGT CTG ATG ATG-3' (sense), 5'-GGC AAT GCG GTT CTG ATA CTG-3' (anti-sense); mouse GAPDH (as an internal control for PCR), 5'-CAA TGC CAA GTA TGA TGA CAT-3' (sense), 5'-CCT GTT ATT ATG GGG TCC TG-3' (anti-sense).

3.9. Preparation of Whole-Cell, Cytoxolic, and Nuclear Extracts

RAW 264.7 cells grown at 2×10^5 cells/well in 6-well plates were stimulated with RMO for 1 h following pretreatment in the presence of absence of 1 μg/mL LPS for various time periods. Whole-cell extracts were then prepared according to the manufacturer's instructions using Cell lysis Buffer containing 20 mM Tris (pH 7.5), 135 mM NaCl, 2 mM EDTA, 2 mM DTT, 25 mM β-glycerophosphate, 2 mM sodium pyrophosphate, 10% glycerol, 1% Triton X-100, 1 mM sodium orthovanadate, 10 mM NaF, 10 μg/mL aprotinin, 10 μg/mL leupeptin, and 1 mM PMSF. The cytosolic and nuclear extracts were prepared as above using a kit (Pierce Biotechnology Inc, Rockford, IL, USA). The protein content was quantified by absorbance at 590 nm according to the BCA protein assay (Pierce Biotechnology).

3.10. Western Blot Analysis

Proteins (whole-cell extracts: 30 μg/lane, nuclear extracts: 10 μg/lane, cytosolic extracts: 30 μg/lane) were separated by electrophoresed on a 10% SDS-polyacrylamide gel, and transferred to PVDF membranes with a semidry transfer system (Bio-Rad). The membranes were blocked with 5% nonfat milk in PBST with 0.1% Tween 20 for 1 h at room temperature, and then incubated overnight with primary antibodies. After hybridization with primary antibodies, the membrane was washed five times with PBST for 5 min, then incubated with horseradish peroxidase-conjugated secondary antibody for 1 h at RT and washed five times with PBST for 5 min. Final detection was performed with Western Blotting Luminol reagents (SantaCruz Biotechnology, Santa Cruz, CA, USA). Monoclonal antibodies against IKK β, p-IκBα, IκBα, p-NFκB-p65, and ERK and polyclonal antibodies against TNF-α, NFκB-p65, p-IKK α/β, p-EKR, p-p38, p38, p-SAPK/JNK, SAPK/JNK, IKKα, p-MEK1/2, p-MKK3/MKK6, p-B-Raf, MLK3, SEK1/MKK4, p-MKK7, p-ASK1 and p-TAK1 were purchased from Cell Signaling Technology, Inc. (Beverly, MA, USA). The polyclonal antibodies against iNOS, COX-2, IL-1 β, IL-6, Lamin B and β -actin were purchased from Santa Cruz Biotechnology, Inc.

3.11. Confocal Microscopy Analysis

RAW264.7 cells were planted on the coverglass bottom dishes. After 24 h, the cells (2×10^5 cells/well) were pretreated with 100 μg/mL RMO for 2 h and then stimulated with 1 μg/mL LPS for 1 h. The cells were fixed with 4% paraformaldehyde for 10 min, permeabilized with 0.2% Triton X-100 for 10 min, blocked with 3% BSA in PBS for 2 h, incubated with an anti-p65 primary antibody at room temperature for 2 h, sequentially incubated with an Alexa Fluor 555-conjugated secondary antibody (Cell Signaling) at room temperature for 2 h in the dark, and finally incubated with 1 μg/mL of 4',6'-diamidino-2-phenylindole (DAPI) at room temperature for 20 min in the dark. Images were obtained using a LSM 510 laser confocal microscope (Zeiss, Jena, Germany).

3.12. Analysis of Phytosterol Content

Ten g of RMO were saponified in a round-bottom flask containing 0.1 N ethanolic KOH (10 mL) and ethanol (40 mL). The mixture was refluxed for 1 h on a heating mantle at 95 °C. After saponification, the mixture was cooled to room temperature, mixed with saturated NaOH solution (50 mL) and transferred to a separatory funnel. The unsaponifiables were extracted 4 times with 100-mL portions of hexane. The combined hexane extracts were concentrated to dryness using a rotary evaporator and 25 mL of an internal standard solution (5α-cholestane, 1 mg/mL) was added to the concentrate. The unsaponifiables were analyzed by an Agilent 6890 gas chromatograph (Agilent Technologies, Santa Clara, CA, USA) equipped with a DB5 MS column (Agilent) and a flame ionization detector. The column temperature was programmed from 200 °C for 2 min, 200 °C to 300 °C at 5 °C/min, and held for 5 min. Nitrogen gas was the carrier gas at a flow rate of 3 mL/min and the spilt ratio was 10:1. The injection port and the detector temperatures were 270 °C and 300 °C, respectively.

3.13. Statistical Analysis

The data were expressed as mean ± S.D. values. The values were compared with the control using analysis of variance followed by unpaired Student's t tests. A *p* value of <0.05 was considered significant.

4. Conclusions

RMO suppressed the LPS-stimulated inflammatory responses including NO and PGE2 generation, secretion of *pro*-inflammatory cytokines of TNF-α, IL-1β and IL-6 and the expression of *pro*-inflammatory mediators such as iNOS and COX-2 in RAW264.7 macrophages. Furthermore, RMO enhanced the inhibitory effects on inflammation via inactivation of NFκB and p38/ MKK3/6/TAK1 signaling pathways. RMO contained about 10% phytosterols including sitosterol, stigmasterol and campesterol which may contribute to the anti-inflammatory properties of RMO. Taken together, our data suggest that RMO might exert its anti-inflammatory ability through inhibiting p38 pathway which leads to NFκB inactivation and thereby suppressing expressions of inflammatory target proteins including proinflammatory cytokines and enzymes. Our findings suggest for the first time the potential of red ginseng marc oil as a potent natural anti-inflammatory agent.

Acknowledgments

References

1. Chung, H.Y.; Cesari, M.; Anton, S.; Marzetti, E.; Giovannini, S.; Seo, A.Y.; Carter, C.; Yu, B.P.; Leeuwenburgh, C. Molecular inflammation: Underpinnings of aging and age-related diseases. *Ageing Res. Rev.* **2009**, *8*, 18–30.
2. Chen, S.R.; Xu, X.Z.; Wang, Y.H.; Chen, J.W.; Xu, S.W.; Gu, L.Q.; Liu, P.Q. Icariin derivative inhibits inflammation through suppression of p38 mitogen-activated protein kinase and nuclear factor-kappaB pathways. *Biol. Pharm. Bull.* **2011**, *33*, 1307–1313.
3. Uto, T.; Suangkaew, N.; Morinaga, O.; Kariyazono, H.; Oiso, S.; Shoyama, Y. Eriobotryae folium extract suppresses LPS-induced iNOS and COX-2 expression by inhibition of NF-kappaB and MAPK activation in murine macrophages. *Am. J. Chin. Med.* **2011**, *38*, 985–994.
4. Sethi, G.; Sung, B.; Aggarwal, B.B. Nuclear factor-kappaB activation: From bench to bedside. *Exp. Biol. Med. (Maywood)* **2008**, *233*, 21–31.
5. Guha, M.; Mackman, N. LPS induction of gene expression in human monocytes. *Cell. Signal.* **2001**, *13*, 85–94.
6. Yamazaki, Y.; Kawano, Y. Inhibitory effects of herbal alkaloids on the tumor necrosis factor-alpha and nitric oxide production in lipopolysaccharide-stimulated RAW264 macrophages. *Chem. Pharm. Bull. (Tokyo)* **2011**, *59*, 388–391.

7. Lin, C.M.; Huang, S.T.; Liang, Y.C.; Lin, M.S.; Shih, C.M.; Chang, Y.C.; Chen, T.Y.; Chen, C.T. Isovitexin suppresses lipopolysaccharide-mediated inducible nitric oxide synthase through inhibition of NF-kappa B in mouse macrophages. *Planta Med.* **2005**, *71*, 748–753.

8. Shishodia, S.; Potdar, P.; Gairola, C.G.; Aggarwal, B.B. Curcumin (diferuloylmethane) down-regulates cigarette smoke-induced NF-kappaB activation through inhibition of IkappaBalpha kinase in human lung epithelial cells: Correlation with suppression of COX-2, MMP-9 and cyclin D1. *Carcinogenesis* **2003**, *24*, 1269–1279.

9. Song, S.H.; Min, H.Y.; Han, A.R.; Nam, J.W.; Seo, E.K.; Park, S.W.; Lee, S.H.; Lee, S.K. Suppression of inducible nitric oxide synthase by (−)-isoeleutherin from the bulbs of Eleutherine americana through the regulation of NF-kappaB activity. *Int. Immunopharmacol.* **2009**, *9*, 298–302.

10. Saklatvala, J. Inflammatory signaling in cartilage: MAPK and NF-kappaB pathways in chondrocytes and the use of inhibitors for research into pathogenesis and therapy of osteoarthritis. *Curr. Drug Targets* **2007**, *8*, 305–313.

11. Vanden Berghe, W.; Plaisance, S.; Boone, E.; de Bosscher, K.; Schmitz, M.L.; Fiers, W.; Haegeman, G. p38 and extracellular signal-regulated kinase mitogen-activated protein kinase pathways are required for nuclear factor-kappaB p65 transactivation mediated by tumor necrosis factor. *J. Biol. Chem.* **1998**, *273*, 3285–3290.

12. Kyriakis, J.M.; Avruch, J. Mammalian mitogen-activated protein kinase signal transduction pathways activated by stress and inflammation. *Physiol. Rev.* **2001**, *81*, 807–869.

13. Yoon, W.J.; Moon, J.Y.; Song, G.; Lee, Y.K.; Han, M.S.; Lee, J.S.; Ihm, B.S.; Lee, W.J.; Lee, N.H.; Hyun, C.G. Artemisia fukudo essential oil attenuates LPS-induced inflammation by suppressing NF-kappaB and MAPK activation in RAW 264.7 macrophages. *Food Chem. Toxicol.* **2010**, *48*, 1222–1229.

14. Kim, J.Y.; Shin, J.S.; Ryu, J.H.; Kim, S.Y.; Cho, Y.W.; Choi, J.H.; Lee, K.T. Anti-inflammatory effect of anemarsaponin B isolated from the rhizomes of Anemarrhena asphodeloides in LPS-induced RAW 264.7 macrophages is mediated by negative regulation of the nuclear factor-kappaB and p38 pathways. *Food Chem. Toxicol.* **2009**, *47*, 1610–1617.

15. Kim, Y.J.; Kim, H.C.; Ko, H.; Amor, E.C.; Lee, J.W.; Yang, H.O. Stercurensin inhibits nuclear factor-kappaB-dependent inflammatory signals through attenuation of TAK1-TAB1 complex formation. *J. Cell. Biochem.* **2011**, *112*, 548–558.

16. Jang, D.J.; Lee, M.S.; Shin, B.C.; Lee, Y.C.; Ernst, E. Red ginseng for treating erectile dysfunction: A systematic review. *Br. J. Clin. Pharmacol.* **2008**, *66*, 444–450.

17. Kim, J.Y.; Kim, J.J.; Kim, H.J. Effect of Oral Administration of Korean Red Ginseng on Influenza A (H1N1) Virus Infection *J. Ginseng Res.* **2011**, *35*, 104–110.

18. Park, B.J.; Lim, Y.S.; Lee, H.J.; Eum, W.S.; Park, J.; Han, K.H.; Choi, S.Y.; Lee, K.S. Anti-oxidative effects of Phellinus linteus and red ginseng extracts on oxidative stress-induced DNA damage. *BMB Rep.* **2009**, *42*, 500–505.

19. Hwang, J.T.; Lee, M.S.; Kim, H.J.; Sung, M.J.; Kim, H.Y.; Kim, M.S.; Kwon, D.Y. Antiobesity effect of ginsenoside Rg3 involves the AMPK and PPAR-gamma signal pathways. *Phytother. Res.* **2009**, *23*, 262–266.

20. Seo, E.Y.; Kim, W.K. Red Ginseng Extract Reduced Metastasis of Colon Cancer Cells *In Vitro* and *In Vivo*. *J. Ginseng Res.* **2011**, *35*, 315–324.

21. Abdel-Aziem, S.H.; Mosaad, A.; Gamil, K.; El-Kady, A.A.; El-Nekeety, A.A.; Nam, K.W. Therapeutic Effects of Korean Red Ginseng Extract in Egyptian Patients with Chronic Liver Diseases. *J. Ginseng Res.* **2011**, *35*, 69–79.

22. Alexopoulos, A.; Kimbaris, A.C.; Plessas, S.; Mantzourani, I.; Theodoridou, I.; Stavropoulou, E.; Polissiou, M.G.; Bezirtzoglou, E. Antibacterial activities of essential oils from eight Greek aromatic plants against clinical isolates of Staphylococcus aureus. *Anaerobe* **2011**, *17*, 399–402.

23. Waikedre, J.; Vitturo, C.I.; Molina, A.; Theodoro, P.N.; do Rosario Rodrigues Silva, M.; Espindola, L.S.; Maciuk, A.; Fournet, A. Antifungal Activity of the Essential Oils of Callitris neocaledonica and *C. sulcata* Heartwood (Cupressaceae). *Chem. Biodivers.* **2012**, *9*, 644–653.

24. Kim, H.J.; Kang, H.J.; Seo, J.Y.; Lee, C.H.; Kim, Y.S.; Kim, J.S. Antiobesity effect of oil extract of ginseng. *J. Med. Food* **2011**, *14*, 573–583.

25. Sindhu, S.; Chempakam, B.; Leela, N.K.; Suseela Bhai, R. Chemoprevention by essential oil of turmeric leaves (Curcuma longa L.) on the growth of Aspergillus flavus and aflatoxin production. *Food Chem. Toxicol.* **2011**, *49*, 1188–1192.

26. Yoon, W.J.; Moon, J.Y.; Kang, J.Y.; Kim, G.O.; Lee, N.H.; Hyun, C.G. Neolitsea sericea essential oil attenuates LPS-induced inflammation in RAW 264.7 macrophages by suppressing NF-kappaB and MAPK activation. *Nat. Prod. Commun.* **2010**, *5*, 1311–1316.

27. Bak, M.J.; Jun, M.; Jeong, W.S. Antioxidant and Hepatoprotective Effects of the Red Ginseng Essential Oil in H(2)O(2)-Treated HepG2 Cells and CCl(4)-Treated Mice. *Int. J. Mol. Sci.* **2011**, *13*, 2314–2330.

28. Surh, Y.J.; Chun, K.S.; Cha, H.H.; Han, S.S.; Keum, Y.S.; Park, K.K.; Lee, S.S. Molecular mechanisms underlying chemopreventive activities of anti-inflammatory phytochemicals: Down-regulation of COX-2 and iNOS through suppression of NF-kappa B activation. *Mutat. Res.* **2001**, *480–481*, 243–268.

29. Pan, M.H.; Lai, C.S.; Dushenkov, S.; Ho, C.T. Modulation of inflammatory genes by natural dietary bioactive compounds. *J. Agric. Food Chem.* **2009**, *57*, 4467–4477.

30. Aggarwal, B.B.; Shishodia, S.; Sandur, S.K.; Pandey, M.K.; Sethi, G. Inflammation and cancer: How hot is the link? *Biochem. Pharmacol.* **2006**, *72*, 1605–1621.

31. Korhonen, R.; Lahti, A.; Kankaanranta, H.; Moilanen, E. Nitric oxide production and signaling in inflammation. *Curr. Drug Targets Inflamm. Allergy* **2005**, *4*, 471–479.

32. Feldmann, M. Many cytokines are very useful therapeutic targets in disease. *J. Clin. Invest.* **2008**, *118*, 3533–3536.

33. Ren, K.; Torres, R. Role of interleukin-1beta during pain and inflammation. *Brain Res. Rev.* **2009**, *60*, 57–64.

34. Sugita, T. Targeting therapy for inflammatory diseases by anti-TNFalpha biologics. *Yakugaku Zasshi* **2009**, *129*, 19–24.

35. Ding, C.; Cicuttini, F.; Li, J.; Jones, G. Targeting IL-6 in the treatment of inflammatory and autoimmune diseases. *Expert Opin. Investig. Drugs* **2009**, *18*, 1457–1466.

36. Medzhitov, R.; Horng, T. Transcriptional control of the inflammatory response. *Nat. Rev. Immunol.* **2009**, *9*, 692–703.

37. Ghosh, S.; Hayden, M.S. New regulators of NF-kappaB in inflammation. *Nat. Rev. Immunol.* **2008**, *8*, 837–848.

38. Akira, S.; Takeda, K. Toll-like receptor signalling. *Nat. Rev. Immunol.* **2004**, *4*, 499–511.

39. Hsieh, I.N.; Chang, A.S.; Teng, C.M.; Chen, C.C.; Yang, C.R. Aciculatin inhibits lipopolysaccharide-mediated inducible nitric oxide synthase and cyclooxygenase-2 expression via suppressing NF-kappaB and JNK/p38 MAPK activation pathways. *J. Biomed. Sci.* **2011**, *18*, 28.

40. Baeuerle, P.A.; Henkel, T. Function and activation of NF-kappa B in the immune system. *Annu. Rev. Immunol.* **1994**, *12*, 141–179.

41. Dev, A.; Iyer, S.; Razani, B.; Cheng, G. NF-kappaB and innate immunity. *Curr. Top. Microbiol. Immunol.* **2011**, *349*, 115–143.

42. Jeong, W.S.; Kim, I.W.; Hu, R.; Kong, A.N. Modulatory properties of various natural chemopreventive agents on the activation of NF-kappaB signaling pathway. *Pharm. Res.* **2004**, *21*, 661–670.

43. Kim, C.S.; Kawada, T.; Kim, B.S.; Han, I.S.; Choe, S.Y.; Kurata, T.; Yu, R. Capsaicin exhibits anti-inflammatory property by inhibiting IkB-a degradation in LPS-stimulated peritoneal macrophages. *Cell. Signal.* **2003**, *15*, 299–306.

44. Yadav, P.N.; Liu, Z.; Rafi, M.M. A diarylheptanoid from lesser galangal (Alpinia officinarum) inhibits proinflammatory mediators via inhibition of mitogen-activated protein kinase, p44/42, and transcription factor nuclear factor-kappa B. *J. Pharmacol. Exp. Ther.* **2003**, *305*, 925–931.

45. Bak, M.J.; Jeong, J.H.; Kang, H.S.; Jin, K.S.; Ok, S.; Jeong, W.S. Cedrela sinensis leaves suppress oxidative stress and expressions of iNOS and COX-2 via MAPK signaling pathways in RAW 264.7 cells. *J. Food Sci. Nutr.* **2009**, *14*, 269–276.

46. Costa, G.; Francisco, V.; Lopes, M.C.; Cruz, M.T.; Batista, M.T. Intracellular signaling pathways modulated by phenolic compounds: Application for new anti-inflammatory drugs discovery. *Curr. Med. Chem.* **2012**, *19*, 2876–2900.

47. Johnson, G.L.; Lapadat, R. Mitogen-activated protein kinase pathways mediated by ERK, JNK, and p38 protein kinases. *Science* **2002**, *298*, 1911–1912.

48. Rajapakse, N.; Kim, M.M.; Mendis, E.; Kim, S.K. Inhibition of inducible nitric oxide synthase and cyclooxygenase-2 in lipopolysaccharide-stimulated RAW264.7 cells by carboxybutyrylated glucosamine takes place via down-regulation of mitogen-activated protein kinase-mediated nuclear factor-kappaB signaling. *Immunology* **2008**, *123*, 348–357.

49. Kaminska, B. MAPK signalling pathways as molecular targets for anti-inflammatory therapy—From molecular mechanisms to therapeutic benefits. *Biochim. Biophys. Acta* **2005**, *1754*, 253–262.

50. Pearson, G.; Robinson, F.; Beers Gibson, T.; Xu, B.E.; Karandikar, M.; Berman, K.; Cobb, M.H. Mitogen-activated protein (MAP) kinase pathways: Regulation and physiological functions. *Endocr. Rev.* **2001**, *22*, 153–183.

51. Raingeaud, J.; Whitmarsh, A.J.; Barrett, T.; Derijard, B.; Davis, R.J. MKK3- and MKK6-regulated gene expression is mediated by the p38 mitogen-activated protein kinase signal transduction pathway. *Mol. Cell. Biol.* **1996**, *16*, 1247–1255.

52. Cho, S.Y.; Park, S.J.; Kwon, M.J.; Jeong, T.S.; Bok, S.H.; Choi, W.Y.; Jeong, W.I.; Ryu, S.Y.; Do, S.H.; Lee, C.S.; *et al*. Quercetin suppresses proinflammatory cytokines production through MAP kinases andNF-kappaB pathway in lipopolysaccharide-stimulated macrophage. *Mol. Cell. Biochem.* **2003**, *243*, 153–160.

53. Lo, A.H.; Liang, Y.C.; Lin-Shiau, S.Y.; Ho, C.T.; Lin, J.K. Carnosol, an antioxidant in rosemary, suppresses inducible nitric oxide synthase through down-regulating nuclear factor-kappaB in mouse macrophages. *Carcinogenesis* **2002**, *23*, 983–991.

54. Jeong, W.S.; Lachance, P.A. Phytosterols and Fatty Acids in Fig (*Ficus carica*, var. Mission) Fruit and Tree Components. *J. Food Sci.* **2001**, *66*, 278–281.

55. Othman, R.A.; Moghadasian, M.H. Beyond cholesterol-lowering effects of plant sterols: Clinical and experimental evidence of anti-inflammatory properties. *Nutr. Rev.* **2011**, *69*, 371–382.

56. Zhao, Y.Q.; Yuan, C.L. Chemical constituents of the fruit of *Panax ginseng* C. A. Meyer. *Zhongguo Zhong Yao Za Zhi* **1993**, *18*, 296–297, 319.

57. Beveridge, T.H.; Li, T.S.; Drover, J.C. Phytosterol content in American ginseng seed oil. *J. Agric. Food Chem.* **2002**, *50*, 744–750.

Sample Availability: Samples of the red ginseng marc oil are available from the authors.